Beam wandering statistics of twin thin laser beam propagation under generalized atmospheric conditions

Darío G. Pérez[1,*] **and Gustavo Funes**[2]

[1]*Instituto de Física, Facultad de Ciencias, Pontificia Universidad Católica de Valparaíso (PUCV), Av. Brasil 2950, 23-40025 Valparaíso, Chile*

[2]*Centro de Investigaciones Ópticas (CIOp), CC. 124 Correo Central, 1900 La Plata, Argentina*

[*]*dario.perez@ucv.cl*

Abstract: Under the Geometrics Optics approximation is possible to estimate the covariance between the displacements of two thin beams after they have propagated through a turbulent medium. Previous works have concentrated in long propagation distances to provide models for the wandering statistics. These models are useful when the separation between beams is smaller than the propagation path—regardless of the characteristics scales of the turbulence. In this work we give a complete model for these covariances, behavior introducing absolute limits to the validity of former approximations. Moreover, these generalizations are established for non-Kolmogorov atmospheric models.

OCIS codes: (010.1300) Atmospheric propagation; (010.1330) Atmospheric turbulence; (280.4788) Optical sensing and sensors; (280.0280) Remote sensing and sensors.

References and links

1. J. Zhang and Z. Zeng, "Statistical properties of optical turbulence in a convective tank: experimental results," J. Opt. A: Pure Appl. Opt. **3**, 236–241 (2001).
2. C. Innocenti and A. Consortini, "Refractive index gradient of the atmosphere at near ground levels," J. Mod. Optics **52**, 671–689 (2005).
3. J. H. Churnside and R. J. Lataitis, "Angle-of-arrival fluctuations of a reflected beam in atmospheric turbulence," J. Opt. Soc. Am. A **4**, 1264–1272 (1987).
4. E. Masciadri and J. Vernin, "Optical technique for inner-scale measurement: possible astronomical applications," Appl. Opt. **36**, 1320–1327 (1997).
5. M. S. Andreeva, A. V. Koryabin, V. A. Kulikov, and V. I. Shmalhausen, "Diagnostics of the scale of turbulence using a divergent laser beam," Moscow Univ. Phys. Bull. **66**, 627–630 (2011).
6. M. S. Andreeva, N. G. Iroshnikov, A. B. Koryabin, A. V. Larichev, and V. I. Shmalgauzen, "Usage of wave-front sensor for estimation of atmospheric turbulence parameters," Optoelectronics, Instrumentation and Data Processing **48**, 197–204 (2012).
7. A. Consortini and K. O'Donnell, "Beam wandering of thin parallel beams through atmospheric turbulence," Wave. Random Media **3**, S11–S28 (1991).
8. A. Consortini and K. O'Donnell, "Measuring the inner-scale of atmospheric turbulence by correlation of lateral displacements of thin parallel laser beams," Wave. Random Media **3**, S11–S28 (1991).
9. A. Consortini, C. Innocenti, and G. Paoli, "Estimate method for outer scale of atmospheric turbulence," Opt. Comm. **214**, 9–14 (2002).
10. Y. Y. Sun, A. Consortini, and Z. P. Li, "A new method for measuring the outer scale of atmospheric turbulence," Wave. Random Complex **17**, 1–8 (2007).
11. E. Golbraikh and N. S. Kopeika, "Behavior of structure function of refraction coefficients in different turbulent field," Appl. Opt. **43**(33), 6151–6156 (2004).

#175466 - $15.00 USD Received 4 Sep 2012; revised 4 Nov 2012; accepted 15 Nov 2012; published 29 Nov 2012

12. E. Golbraikh, H. Branover, N. S. Kopeika, and A. Zilberman, "Non-Kolmogorov atmospheric turbulence and optical signal propagation," Nonlin. Processes Geophys. **13**, 297–301 (2006).
13. G. D. Boreman and C. Dainty, "Zernike expansions for non-Kolmogorov turbulence," J. Opt. Soc. Am. A **13**, 517–522 (1996).
14. I. Toselli, L. C. Andrews, R. L. Phillips, and V. Ferrero, "Angle of arrival fluctuations for free space laser beam propagation through non-Kolmogorov turbulence," Proc. SPIE **6551**, 65510E (2007).
15. C. Rao, W. Jiang, and N. Ling, "Atmospheric characterization with Shack-Hartmann wavefront sensors for non-Kolmogorov turbulence," Opt. Eng. **41**(2), 534–541 (2002).
16. P. F. Lazorenko, "Differential image motion at non-Kolmogorov distortions of the turbulent wave-front," Astron. Astrophys. **382**, 1125–1137 (2002).
17. P. F. Lazorenko, "Non-Kolmogorov features of differential image motion restored from the Multichannel Astrometric Photometer data," Astron. Astrophys. **396**, 353–360 (2002).
18. E. Golbraikh and N. S. Kopeika, "Turbulence strength parameter in laboratory and natural optical experiments in non-Kolmogorov cases," Opt. Commun. **242**, 333–338 (2004).
19. A. Zilberman, E. Golbraikh, and N. S. Kopeika, "Some limitations on optical communication reliability through Kolmogorov and non-Kolmogorov turbulence," Opt. Commun.**283**, 1229–1235 (2010).
20. L. Zunino, D. G. Pérez, O. A. Rosso, and M. Garavaglia, "Characterization of Laser Propagation Through Turbulent Media by Quantifiers Based on the Wavelet Transform," Fractals **12**, 223–233 (2004).
21. D. G. Pérez, L. Zunino, M. Garavaglia, and D. G. Pérez, "A fractional Brownian motion model for the turbulent refractive index in lightwave propagation," Opt. Commun. **242**, 57–63 (2004).
22. D. G. Pérez, L. Zunino, and M. Garavaglia, "Modeling the turbulent wave-front phase as a fractional Brownian motion: a new approach," J. Opt. Soc. Am. A **21**, 1962–1969 (2004).
23. D. G. Pérez and L. Zunino, "Generalized wave-front phase for non-Kolmogorov turbulence," Opt. Lett. **33**, 572–574 (2008).
24. L. Zunino, D. G. Pérez, M. Garavaglia, O. A. Rosso, and D. G. Pérez, "Characterization of laser propagation through turbulent media by quantifiers based on the wavelet transform: dynamic study," Physica A **364**, 79–86 (2006).
25. G. Funes, D. D. Gulich, L. Zunino, D. G. Pérez, M. Garavaglia, and D. G. Pérez, "Behavior of the laser beam wandering variance with the turbulent path length," Opt. Commun. **272**, 476–479 (2007).
26. D. D. Gulich, G. Funes, L. Zunino, D. G. Pérez, and M. Garavaglia, "Angle-of-arrival variance's dependence on the aperture size for indoor convective turbulence," Opt. Commun. **277**, 241–246 (2007).
27. P. Beckman, "Signal Degeneration in Laser Beams Propagated Through a Turbulent atmosphere," Radio Sci. J. Res. (NBS/USNC-URSI) **69D**, 629–640 (1965).
28. Equations (1) and (2) are obtained in [7] from approximating the beam displacements through Geometric Optics. Since there is a linear relationship between these displacements and the refractive index perturbation, through integrals and derivatives, their covariances are functionals of it. This is true regardless of the model employed to evaluate the covariance of the turbulent refractive index.
29. V. I. Tatarskiĭ, *Wave Propagation in a Turbulent Atmosphere* (Nauka Press, Moscow, 1967).
30. L. C. Andrews and R. L. Phillips, *Laser Beam Propagation through Random Media* (SPIE, 1998).
31. C. Innocenti and A. Consortini, "Estimate of characteristic scales of atmospheric turbulence by thin beams: Comparison between the von Karman and Hill-Andrews models," J. Mod. Optics **51**(3), 333-342 (2004).
32. D. G. Pérez, A. Férnandez, G. Funes, D. Gulich, and L. Zunino, "Retrieving atmospheric turbulence features from differential laser tracking motion data," Proc. SPIE **8535**, 853508 (2012).

1. Introduction

As a result of the fluctuating nature of the refractive index in a turbulent medium any laser beam that propagates through it experiments deflections. These displacements are always perpendicular to the initial unperturbed direction of propagation, and arise from the beam phase fluctuations. This phenomenon is commonly known as laser beam wandering because of the dancing the beam performs over a screen. Since it is very sensitive to the turbulence behaviour, it has been used in different experimental configurations to measure the characteristic scales and parameters associated to the turbulence.

For example, single beam wandering experiments have been applied to estimate the coherence length, and turbulence spectrum power-law, through the angle-of-arrival fluctuations variance [1] in a convective water tank. Also, laser beam wandering was used to estimate refractive index gradient variations at near ground levels [2]. But the wander of a single laser beam alone is scant for obtaining all the optical characteristics of a turbulent medium. Therefore, several

#175466 - $15.00 USD Received 4 Sep 2012; revised 4 Nov 2012; accepted 15 Nov 2012; published 29 Nov 2012

papers discuss the determination of these characteristics by studying the angle-of-arrival at two pupils (DIMM configuration) or several pupils [3–6]—usually employing a Shack-Hartmann pupil decomposition. Experimentally the use of a Shack-Hartman sensor, or other multiple pupil devices, is very common; nevertheless, this often requires complex and costly setups.

Consortini and O'Donnell [7,8] introduced a simpler technique, and therefore less expensive, capable of capturing several parameters of the optical turbulence. They developed a Geometric Optics (GO) model for the propagation of twin thin-beams through a turbulent media; particularly, for their covariances. Experimental measurements of these correlations allowed the determination of the inner-, ℓ_0, and outer-scale, L_0, of turbulent media. Further improvements on this method provided alternative estimations of the outer-scale [9, 10]. This technique is specifically useful when studying ground level propagation.

These works were circumscribed to models for Obukhov-Kolmogorov turbulence, but through the years the presence of deviations from these models have been determined; specifically, for ground-level turbulence, where this technique can be easily deployed—see [11, 12] and references therein. Some authors have discussed the theoretical implications of non-Kolmogorov power-spectra in Shack-Hartmann or DIMM arrangements [13, 14], experiments have been performed [12, 15–19] and confirmed deviations under varied conditions.

Under the need to introduce more general statistical descriptions for the turbulent refractive index, we have previously introduced Lévy fractional Brownian fields [20–23] to describe the phase corrugations, and thus the angle-of-arrival. Also, experiments performed by us, on laser beam wandering and wave-front propagation have shown the presence of memory effects reflected in some statistical quantifiers. Such as the wavelet entropy and Hurst exponent [24–26], the latter, we have shown, is proportional to the power exponent in the non-Kolmogorov wave-front phase [23].

The purpose of the present work is to develop a complete model for the propagation of twin-beams in the GO approximation under the influence of non-Kolmogorov turbulence. We start

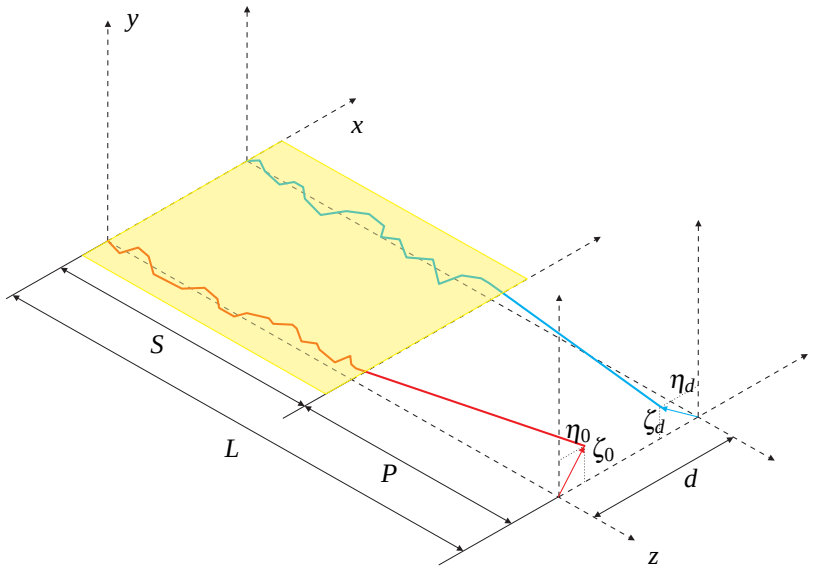

Fig. 1. Two parallels thin beams propagating in a turbulent media. The turbulent region is confined to the zone of length S, after that the beams propagate in a region of length P without being deflected. Originally, the beams are separated a distance d, and the arrival position with respect to the original trajectory is given by (η_0, ζ_0) and (η_d, ζ_d).

#175466 - $15.00 USD Received 4 Sep 2012; revised 4 Nov 2012; accepted 15 Nov 2012; published 29 Nov 2012

with the theory developed in [7] and review the conditions of validity for the long path approximation introduced therein. This theory is used by Consortini *et al.* to obtain analytical results, and is also used in their subsequent works. Later, we describe a non-Kolmogorov model valid for any propagation distance. Specifically, we are mostly interested in short path propagation: a condition frequently observed in the laboratory.

2. The Geometrical Optics approximation for thin beams: basics

Beckmann [27] was able to model the displacement of a thin laser beam in the limits of Geometrical Optics—whenever $\ell_0 \gg \sqrt{L\lambda}$ is achieved; nevertheless, he did so by employing an artificial covariance function far from the Obukhov-Kolmogorov (OK) theoretical model. Consortini & O'Donnell [7,8] established the statistics for a thin-beam propagation under the latter. That is, given two beams propagating (partially) across a turbulent region, Fig. 1, with beam displacements at position d defined by $\eta_d = x_d - \langle x_d \rangle$ and $\zeta_d = y_d - \langle y_d \rangle$, and at the origin by $\eta_0 = x_0 - \langle x_0 \rangle$ and $\zeta_0 = y_0 - \langle y_0 \rangle$, then

$$B_y(d) = \langle \zeta_d \, \zeta_0 \rangle = \int_0^L F\,(z,S,P)\, g_n(z,d)\, dz \tag{1}$$

is the *off-plane covariance* describing displacements perpendicular to the plane containing the propagation axis, z, and the line joining the displacements centres, d; likewise, the *on-plane covariance* is given by

$$B_x(d) = \langle \eta_d \, \eta_0 \rangle = \int_0^L F\,(z,S,P)\, f_n(z,d)\, dz, \tag{2}$$

since the displacements are along the axis defined by d. Here

$$F\,(z,S,P) = 2\left(\frac{S^3}{3} + PS^2 + SP^2\right) - z\left(S^2 + 2PS + 2P^2\right) + \frac{z^3}{3} \tag{3}$$

is the *filter function* moderating the contributions of both the region where the turbulence is active, S, and where it is inactive, P—here $S+P=L$. While the action of the turbulence itself in each axis along the direction of propagation is

$$f_n(z,d) = (2\pi)^{3/2} \int_0^\infty \kappa \Phi_n(\kappa) \left[\frac{\kappa^{3/2} J_{3/2}(\kappa r)}{r^{3/2}} - \frac{d^2 \kappa^{5/2} J_{5/2}(\kappa r)}{r^{5/2}}\right] d\kappa \tag{4}$$

$$g_n(z,d) = (2\pi)^{3/2} \int_0^\infty \kappa \Phi_n(\kappa) \left[\frac{\kappa^{3/2} J_{3/2}(\kappa r)}{r^{3/2}}\right] d\kappa, \tag{5}$$

where $r^2 = z^2 + d^2$, and Φ_n is the spectrum of structure function for the refractive index fluctuations [28]. As discussed by Tatarskĭ [29] the action of dissipative range in the spectrum is best modeled by a decaying exponential function, severing almost any contribution after the inner-scale cut-off $\kappa_m = 2\pi/\ell_0$. For instance, the propagation of two parallel thin beams introduces two distances that can be modified independently, L and d; therefore, the expressions above for each beam covariances should be functions of adimensional magnitudes derived, at least, from these three quantities. Finally, the covariance along the off-plane axis is written

$$B_y(d) = L_m^{5/2} \left[\int_0^1 \tilde{g}_n(u,\delta)\left(\frac{2}{3} - u + \frac{u^3}{3}\right) du - p^2 \int_0^1 \tilde{g}_n(u,\delta)\left(u + \frac{2}{3}p\right) du\right], \tag{6}$$

#175466 - $15.00 USD Received 4 Sep 2012; revised 4 Nov 2012; accepted 15 Nov 2012; published 29 Nov 2012

with $p = P/L$ the fraction of inactive turbulence in the path of length L, $L_m = \kappa_m L$ represents the adimensional propagation distance, and

$$\tilde{g}_n(u,\delta) = (2\pi)^{3/2} \int_0^\infty [\kappa_m k \Phi_n(\kappa_m k)] \left[\frac{k^{3/2} J_{3/2}\left(kL_m\sqrt{u^2+\delta^2}\right)}{(u^2+\delta^2)^{3/4}} \right] dk \tag{7}$$

where $\delta = d/L$ is the separation between beams relative to the propagation distance, the *relative separation*. Since Eq. (4) is functionally dependent of g_n, we define instead *covariance difference*

$$\begin{aligned} \Delta(d) &= B_y(d) - B_x(d) = \\ &= \delta^2 L_m^{7/2} \left[\int_0^1 \tilde{h}_n(u,\delta) \left(\frac{2}{3} - u + \frac{u^3}{3} \right) du \; - p^2 \int_0^1 \tilde{h}_n(u,\delta) \left(u + \frac{2}{3} p \right) du \right], \end{aligned} \tag{8}$$

with

$$\tilde{h}_n(u,\delta) = (2\pi)^{3/2} \int_0^\infty [\kappa_m k \Phi_n(\kappa_m k)] \left[\frac{k^{5/2} J_{5/2}\left(kL_m\sqrt{u^2+\delta^2}\right)}{(u^2+\delta^2)^{5/4}} \right] dk. \tag{9}$$

Observe that the second term in Eq. (6) can be thought as a correcting term function of p; moreover, when p is small its contribution to the covariance is depreciable. In this way the contribution of a partially filled path seems to have a *lowering* effect on the values of the covariances. In order to organize the information in the best way possible we will leave the analysis of the partially filled path to a future work.

3. Twin beam covariance behaviour for generalized spectra for filled paths

3.1. The non-Kolmogorov spectrum case

The non-Kolmogorov spectrum is obtained from a self-similar Lévy fractional Brownian field [23]. Any spatial scale is absent, the inner-scale corresponding to dissipation effects is zero, and the outer-scale is infinite as the bath has no boundaries. That is,

$$\Phi_n(\kappa) = \frac{\sin(\pi H)\Gamma(2H+2)}{4\pi^2} C_n^2 \frac{1}{\kappa^{2H+3}}, \quad \text{with} \quad 0 < H \leq 1/3. \tag{10}$$

This spectrum is the only one that gives an analytical solution to the filled path problem, for any distance, as we will see. The range of variation of H is consistent with the normal variation of $2H+3$ near the ground. First we have,

$$g_n(u,\delta) = HC_n^2 \frac{L^{2H-2}}{(\delta^2+u^2)^{1-H}}, \text{ and} \tag{11}$$

$$h_n(u,\delta) = 2H(1-H)C_n^2 \frac{L^{2H-4}}{(\delta^2+u^2)^{2-H}}. \tag{12}$$

Observe that an adimensional version for these functions is inexistent because there are no characteristic scales, i.e.: the spectrum is self-similar. After integrating with the filter function we arrive to the following

$$\begin{aligned} B_y(d) &= HC_n^2 L^{2H+2} \int_0^1 \frac{\left(2/3 - u + u^3/3\right)}{(\delta^2+u^2)^{1-H}} du \\ &= HC_n^2 L^{2H+2} \delta^{2H-2} \left[\tfrac{2}{3} {}_2F_1\left(1-H, \tfrac{1}{2}; \tfrac{3}{2}; -\delta^{-2}\right) + \right. \\ &\left. - \tfrac{1}{2} {}_2F_1\left(1-H, 1; 2; -\delta^{-2}\right) + \tfrac{1}{12} {}_2F_1\left(1-H, 2; 3; -\delta^{-2}\right) \right] \end{aligned} \tag{13}$$

#175466 - $15.00 USD Received 4 Sep 2012; revised 4 Nov 2012; accepted 15 Nov 2012; published 29 Nov 2012

and

$$\begin{aligned}\Delta(d) &= 2H(1-H)C_n^2L^{2H+2}\delta^2\int_0^1 \frac{\left(2/3-u+u^3/3\right)}{\left(\delta^2+u^2\right)^{2-H}}\,du \\ &= 2H(1-H)C_n^2L^{2H+2}\delta^{2H-2}\left[\tfrac{2}{3}\,{}_2F_1\left(2-H,\tfrac{1}{2};\tfrac{3}{2};-\delta^{-2}\right)+\right. \\ &\left.-\tfrac{1}{2}\,{}_2F_1\left(2-H,1;2;-\delta^{-2}\right)+\tfrac{1}{12}\,{}_2F_1\left(2-H,2;3;-\delta^{-2}\right)\right]. \qquad (14)\end{aligned}$$

Both of these expressions diverge asymptotically as δ^{2H-1} in zero since $H<1/2$. This implies an infinite correlation for both axis. On the other hand, the role of the propagation path is merely being an amplifying factor. The most notorious characteristic is the presence of an axis-cut, Fig. 2(b). It is independent on any scale of the turbulent propagation, but the degree of development of the turbulence. An estimation for the cut can be made from fitting the numerical solutions to $B_x(\delta)=0$ for some Hurst exponents: it grows quadratically as H goes to $1/3$ (Fig.2(d)),

$$\delta_0 = 1.945(\pm 0.3735)H^2 + 0.3995(\pm 0.1291)H + 0.0009689(\pm 0.0092). \qquad (15)$$

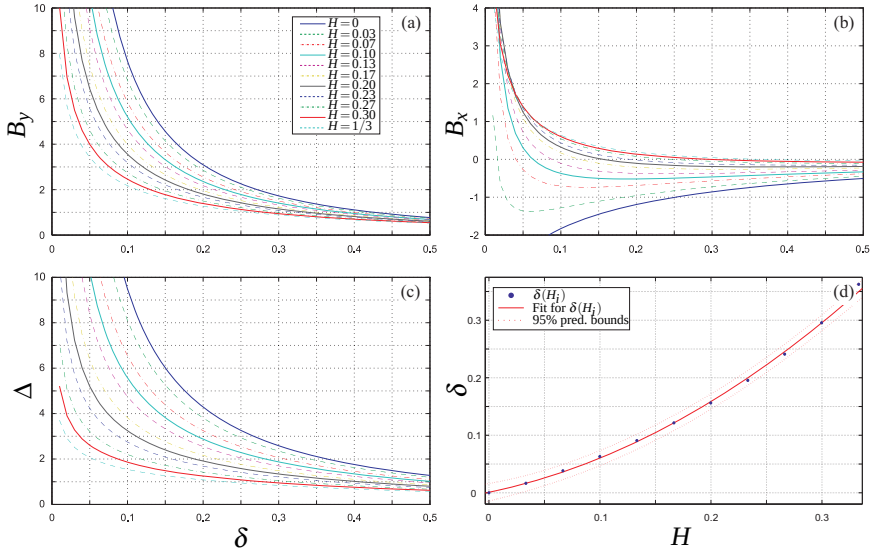

Fig. 2. (a) The off-plane covariance, B_y, is depicted for different values of H. (b) The on-plane covariance, B_x, is shown to cross the δ-axis at different points depending on the value of the Hurst exponent. (c) The covariance difference, Δ, also diverges. (d) The axis cut for the on-plane covariance as a function of the Hurt exponent.

3.2. The (non-K) Tatarskĭ spectrum case

This is the simplest spectrum available considering the effects of the dissipative range. Under the presence of intermittence, and other factors, the spectrum in the inertial range deviates from the Obukhov-Kolmogorov $-11/3$ power exponent; thus, a straightforward extension is

$$\Phi_n(\kappa) = \frac{\sin(\pi H)\Gamma(2H+2)}{4\pi^2}C_n^2\frac{\exp\left(-\kappa^2/\kappa_m^2\right)}{\kappa^{2H+3}}, \quad \text{with} \quad 0<H\leq 1/3. \qquad (16)$$

#175466 - $15.00 USD Received 4 Sep 2012; revised 4 Nov 2012; accepted 15 Nov 2012; published 29 Nov 2012

Evaluating Eqs. (7) and (9) with this spectrum produce analytical results:

$$\tilde{g}_n(u,\delta) = \frac{\sin(\pi H)\Gamma(2H+2)\Gamma(1-H)}{6\pi\kappa_m^{2H+2}} C_n^2 L_m^{3/2}\, {}_1F_1\left[1-H, 5/2, -\frac{L_m^2}{4}\left(\delta^2+u^2\right)\right], \text{ and} \quad (17)$$

$$\tilde{h}_n(u,\delta) = \frac{\sin(\pi H)\Gamma(2H+2)\Gamma(2-H)}{30\pi\kappa_m^{2H+2}} C_n^2 L_m^{5/2}\, {}_1F_1\left[2-H, 7/2, -\frac{L_m^2}{4}\left(\delta^2+u^2\right)\right]. \quad (18)$$

Consortini & O'Donnell [7] discuss this problem only for the OK theory, and their main focus is large propagation paths; however, such situation is hardly found in a laboratory. Moreover, the approximation for the long-propagation path is made without specifying the scale with respect to which the path is longer. For instance, it is suggested in [7] that it must be $L \gg \ell_0$ for the approximation to work—$L_m \gg 1$ for us. Comparing either Eq. (17) or (18) against the filter function F reveals that it is the relative separation, δ, the moderator of whether we are entitled to approximate the filter function or not for the range of L_m achievable under the Geometrical Optics approximation. Effectively, the high ratio required for Consortini's asymptotic approximation is always achievable when tens of meters are compared against a few centimeters of separation between the beams—small relative separations—, but in the laboratory such ratios are usually not possible. Numerical comparison shows uniform convergence from our approach to the asymptotic approximation from [7] given these conditions; nevertheless, observe that local disagreements (such as maxima and roots) may extend further beyond the bounding error between covariances.

First, as a comparison, let us inspect the behaviour of the beams covariances for the OK

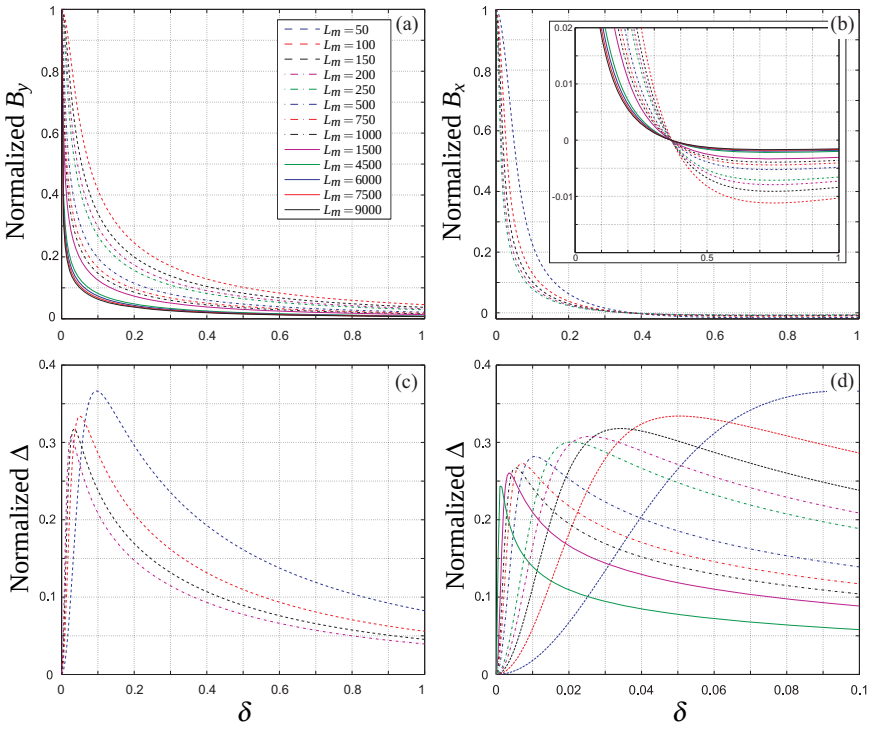

Fig. 3. (a) The normalized off-plane covariance, B_y, is depicted for different values of L_m. (b) The normalized on-plane covariance, B_x, is shown to cross the δ-axis at the same point, $\delta \simeq 0.367$, regardless of the value of L_m. (c) and (d) The normalized covariance difference, Δ, approaches the origin as the adimensional propagation distance increases.

#175466 - $15.00 USD Received 4 Sep 2012; revised 4 Nov 2012; accepted 15 Nov 2012; published 29 Nov 2012

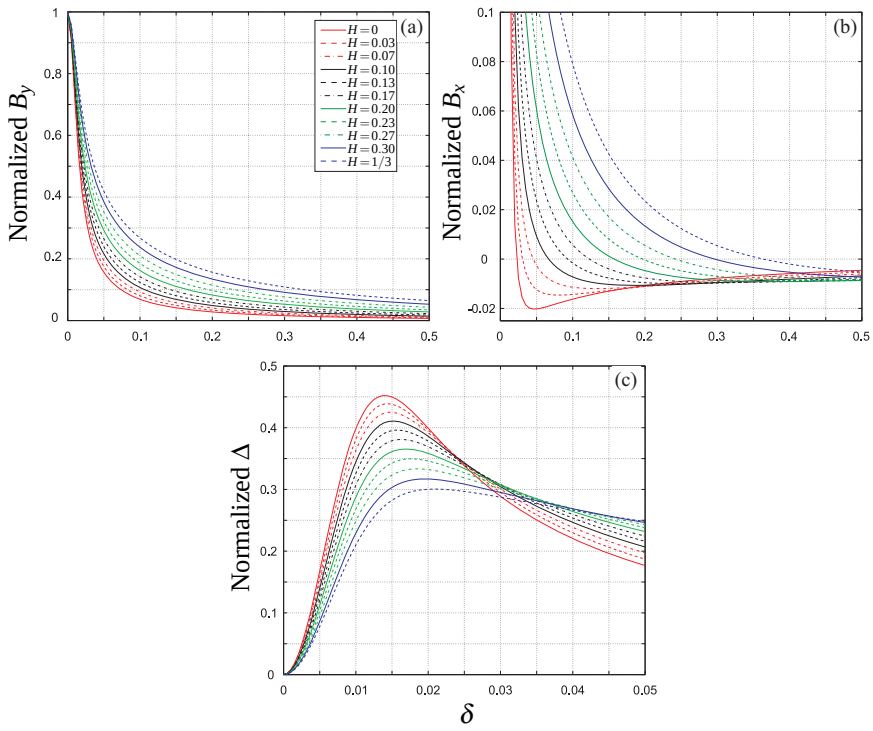

Fig. 4. Fixed the adimensional distance $L_m = 250$: (a) the normalized off-plane covariance for different Hurst exponents becomes rapidly decreasing with lower H; (b) the normalized on-plane covariance axis cut is sensitive to H; (c) the shape of the normalized covariance difference, and its maximum, changes with decreasing H.

theory, i.e., $H = 1/3$. Under the full-path condition, $p = 0$, numerical computation for the on- and off-plane covariances, Eqs. (6) and (8), produces curves similar to those found in [7]. Nevertheless, an axis cut is proved to exists at $\delta \approx 0.367$ for the on-plane covariance, Fig. 3(b), regardless of the value of the inner-scale or the propagation distance. Maximum values for the covariance difference are observed, Fig. 3(d), to decrease its position with the increase in the adimensional propagation distance.

Although, the shape of the covariance function is also modified by the value of the Hurst power exponent, it preserves the same characteristics discussed for the OK model. The off-plane covariance decays as the separation δ increases, and its decay gets sharper as H tends to zero, Fig. 4(a). The on-plane covariance, as expected, decays and cuts the axis at some value that is dependent on H. In opposition to our previous discussion, the degree of development of the turbulence affects the position of the point where the δ-axis is cut—see Fig. 4(b). Again, the Tatarskĭ spectrum also presents an axis-cut, and a partially developed turbulence can show this cut even for long-paths. The difference between off- and on-plane covariances also presents a maximum whose position moves slightly (again) towards zero as H decreases, Fig. 4(c). Bear in mind, that although in both cases—L_m growing or H decreasing—the position of the maximum moves in the same direction, its value and the shape of the curve behave differently: compare Figs. 3(c,d) and 4(c).

For each Hurst power exponent an almost linear relation exists between $2\pi/L_m$ (proportional to the inner-scale when the propagation distance is fixed) and the position of the maximum of Δ. In Fig. 5(top left) we observe this relation, and the occurrence of a departure for small

#175466 - $15.00 USD Received 4 Sep 2012; revised 4 Nov 2012; accepted 15 Nov 2012; published 29 Nov 2012

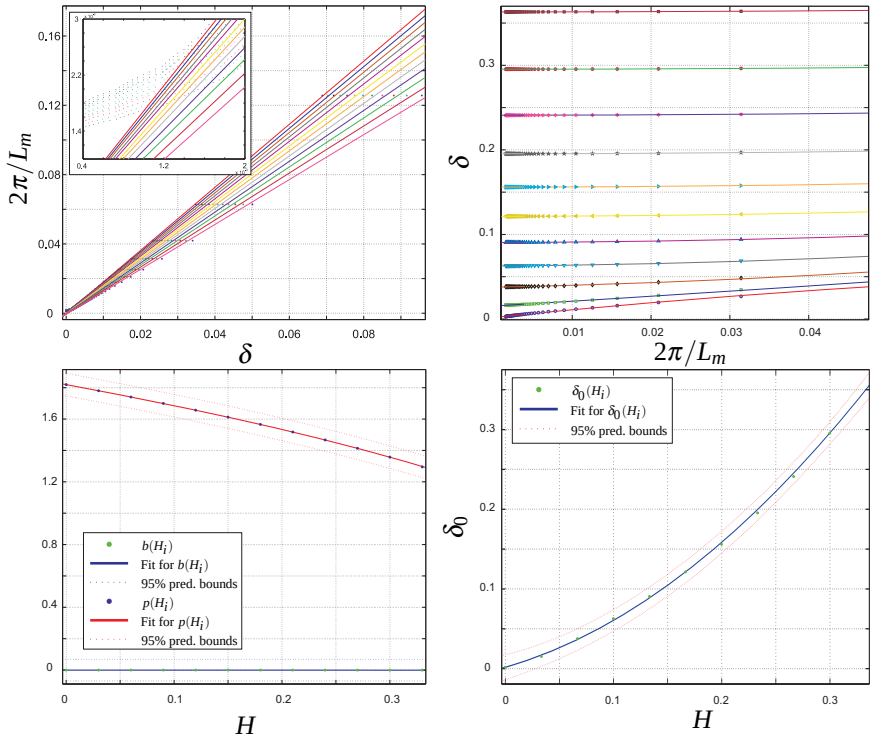

Fig. 5. (top left) $2\pi/L_m$ versus the position of the maximum δ for the difference function; a linear fit is found for most of the range (see zoomed area). The fits giving higher slopes belong to smaller Hurst exponents. (left bottom) Fits coefficients as functions of H; $p(H) = -1.4260(\pm 0.2969)H^3 - 0.4147(\pm 0.1333)H^2 - 1.2890(\pm 0.0157)H + 1.8200(\pm 0.0005)$ and $b(H) = -0.010103(\pm 0.004187)H^3 + 0.000677(\pm 0.001832)H^2 - 0.000442(\pm 0.000209)H - 0.000133(\pm 0.000006)$. (right top) The roots for the on-plane covariance B_x as a function of H. The points corresponds to a numerical evaluation of the covariance's crossing point, then a fit is performed using a quadratic polynomial; $\delta_0(H_i) + \delta_1(H_i)(2\pi/L_m) + \delta_2(H_i)(2\pi/L_m)^2$. (right bottom) Origin ordinate δ_0 as a function of H obtained from the right top fit, Eq (20).

displacements; we can synthesize it as

$$\frac{\ell_0}{2\pi} = p(H)d + b(H)L, \quad \text{for } d < 1.5 \times 10^{-3} L, \tag{19}$$

with $p(H)$ and $b(H)$ given in Fig. 5. The same is true for the on-plane covariance axis-cut, in Fig. 5(right) we observe that these roots are almost unchanged by L_m—only the lowest values of the Hurst exponent produce a root sensitive to the adimensional scale. That is, the inner-scales (and propagation distance) hardly gives us an appreciable change; for propagation distances many times the inner-scale this value is fixed to the origin ordinate fit, $\delta_0(H)$. Thus,

$$\delta_0 = 1.962(\pm 0.3840)H^2 + 0.3915(\pm 0.1328)H + 0.0018(\pm 0.0095). \tag{20}$$

This fit is almost identical to the obtained in the non-Kolmogorov spectrum case, Eq. (15); that is, the inner-scale has little influence in the location of the axis-cut.

#175466 - $15.00 USD Received 4 Sep 2012; revised 4 Nov 2012; accepted 15 Nov 2012; published 29 Nov 2012

3.3. *The (non-K) von Kármán spectrum case*

The generalized (non-Kolmogorov) von Kármán spectrum was introduced by Toselli *et al.* [14]:

$$\Phi_n(\kappa) = \frac{\sin(\pi H)\Gamma(2H+2)}{4\pi^2} C_n^2 \frac{\exp\left(-\kappa^2/\kappa_m^2\right)}{\left(\kappa_0^2+\kappa^2\right)^{H+3/2}}, \quad \text{with} \quad 0 < H \leq 1/3, \tag{21}$$

where $\kappa_0 = 2\pi/L_0$ reflects the effect of the outer-scale for low spatial wave-numbers. In this case analytic representations for both $\tilde{g}_n(u,\delta)$ and $\tilde{f}_n(u,\delta)$ exists as series of Tricomi confluent hypergeometric functions:

$$\tilde{g}_n(u,\delta) = \frac{\sin(\pi H)\Gamma(2H+2)}{\pi^{1/2}2^3\kappa_m^{2+2H}} C_n^2 L_m^{3/2} \sum_{n=0}^{\infty} \frac{(-1)^n}{n!2^{2n}} U\left[\frac{3}{2}+H, H-n; q^2\right] L_m^{2n}\left(\delta^2+u^2\right)^n \tag{22}$$

$$\tilde{h}_n(u,\delta) = \frac{\sin(\pi H)\Gamma(2H+2)}{\pi^{1/2}2^4\kappa_m^{2+2H}} C_n^2 L_m^{5/2} \sum_{n=0}^{\infty} \frac{(-1)^n}{n!2^{2n}} U\left[\frac{3}{2}+H, H-1-n; q^2\right] L_m^{2n}\left(\delta^2+u^2\right)^n, \tag{23}$$

both functions depending on a new adimensional variable $q = \kappa_0/\kappa_m$, the *scale ratio*, besides the other scaling variables defined in the last section. Nevertheless, these series are not uniformly convergent; thus, no analytical integral for the variances exists. However, numerical integration to obtain $\tilde{g}_n$ and $\tilde{h}_n$ from Eqs. (7) and (9) with the von Kármán spectrum, Eq. (21), is possible; moreover, the error can be maintained low enough to proceed with the second integration with the filter function.

The scale ratio manifestation produces some notable changes. Consider $H = 1/3$, suppose we maintain the adimensional distance L_m constant and change the scale ratio; this is equivalent to maintain the inner-scale constant while changing the outer-scale—Fig. 6 illustrates this

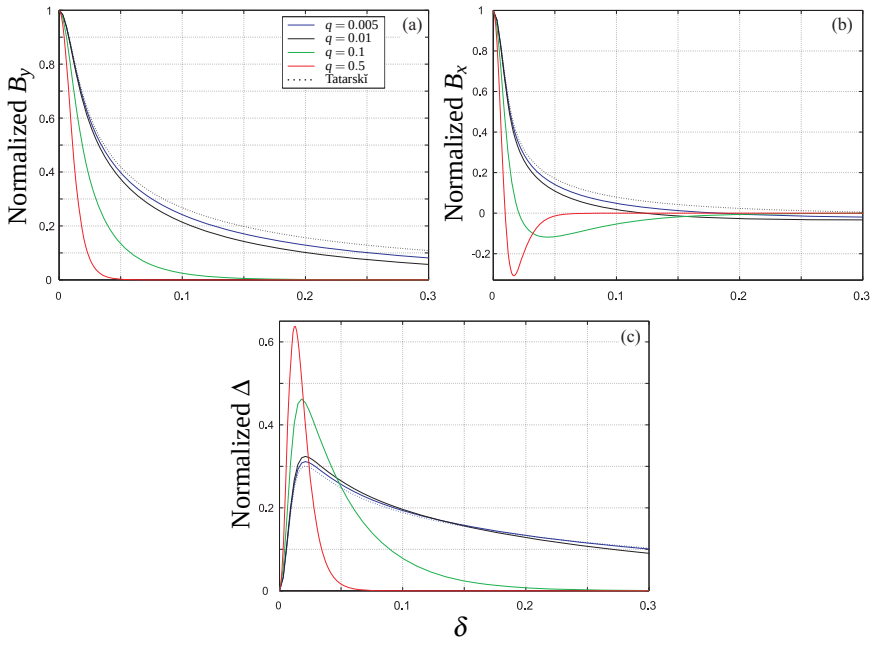

Fig. 6. Fixed the adimensional distance $L_m = 250$, for varying scale ratios compared against the modified Tatarskĭ spectrum case: (a) the normalized off-plane covariance; (b) the normalized on-plane covariance; (c) the normalized covariance difference.

#175466 - $15.00 USD Received 4 Sep 2012; revised 4 Nov 2012; accepted 15 Nov 2012; published 29 Nov 2012

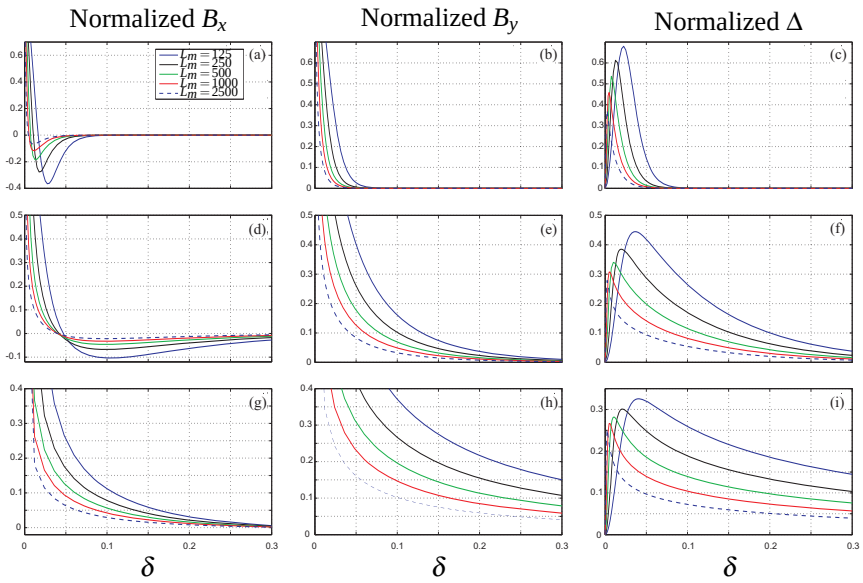

Fig. 7. $m = 100$: (a) normalized on-plane covariance,(b) normalized off-plane covariance, and (c) normalized difference. $m = 10$: (d) normalized on-plane covariance, (e) normalized off-plane covariance, (f) normalized difference. $m = 0.1$: (g) normalized on-plane covariance, (h) normalized off-plane covariance, (i) normalized difference.

case. It is observed that high values of the scale ratio produces notable changes in all covariances shapes, while low q values yields no significative change in their appearance. This is understandable, since physically a fixed L_m can be seen as a fixed inner-scale, high values of the scale ratio are due to outer-scale approaching to the inner-scale. In the limit, that leaves us with no inertial range at all, and all the correlations should occur near the origin. Nevertheless, the effect of even slight changes in the outer-scale affects the axis cut as it is observed in Fig. 6(b), and it is as pronounced as the one produced by the Hurst exponent, Fig. 4. In the covariance difference the maximum is almost indistinguishable from the Tatarskĭ spectrum for relatively moderate q. Here we can observe that the outer-scale somehow affects the position of the maximum but for low values of the scale-ratio this dependence vanishes.

Otherwise, by changing L_m (the inner-scale) and q accordingly it is possible to maintain the outer-scale constant. We define $m = L/L_0$, in Fig. 7 each row is set to a different value of m. Since L would be fixed each row represents a higher value of L_0. Redefining $q = m/L_m$, we observe in the left column of Fig. 7 that the normalized on-plane covariance crosses the horizontal axis further from the origin with higher values of the outer-scale, but along with this the separation between covariances evaluated for different inner-scales coalesce in one crossing point. In the middle column of Fig. 7 we observe the steep of the decrease in the off-plane covariance reduces, being slower with the higher outer-scales. Finally, the position of the maxima of the difference of these covariances change, but is not as noticeable as the properties of each of these alone. Thus, the outer-scale has little influence in the position of the maximum. Since it is the same for all rows in the graphic the maximum should be in the same position. The reason for the deviation in the first row is that the outer-scale is very near the inner-scale.

In the generalized case, we observe—Fig. 8—that the steep of the decreasing of both the on- and off-plane covariances is controlled by the Hurst exponent: with smaller values the slope of descent is increased. This causes the axis-cut to move nearer to the origin, similar to the phenomena we observe for smaller outer-scale but more noticeable. Decreasing values of H

#175466 - $15.00 USD Received 4 Sep 2012; revised 4 Nov 2012; accepted 15 Nov 2012; published 29 Nov 2012

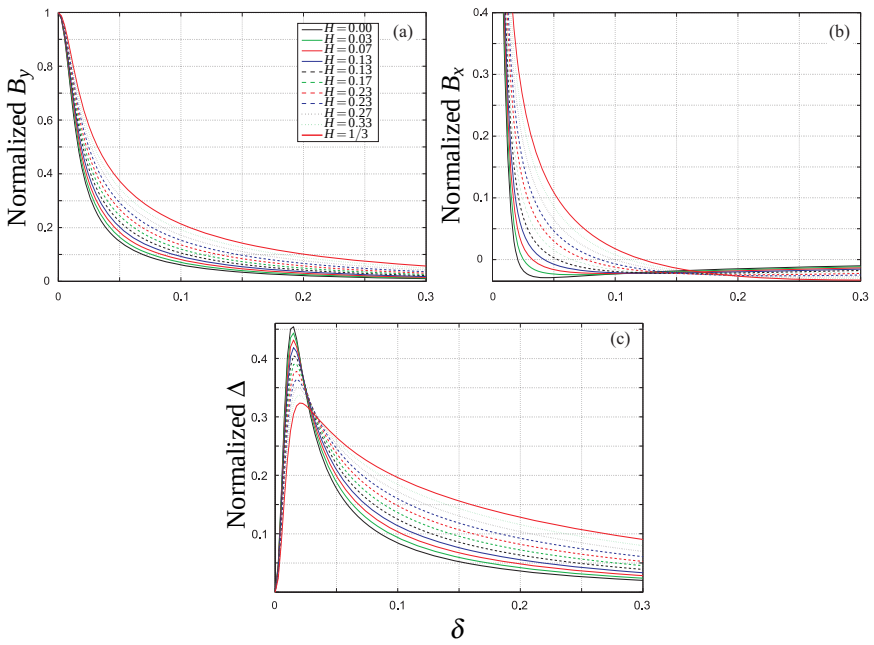

Fig. 8. Fixed the adimensional distance $L_m = 250$ and the scale ratio $q = 0.01$: (a) the normalized off-plane covariance for different Hurst exponents becomes rapidly decreasing with lower H; (b) the normalized on-plane covariance axis cut is sensitive to H; (c) the shape of the normalized covariance difference, and its maximum, changes with decreasing H.

pulls the covariance difference maximum towards the origin, while higher values of the outer-scale (low m) do the opposite, compare Fig. 7 (rightmost column) with Fig. 8(c). The effect of changing the Hurst exponent is the same as in the Tatarskĭ case.

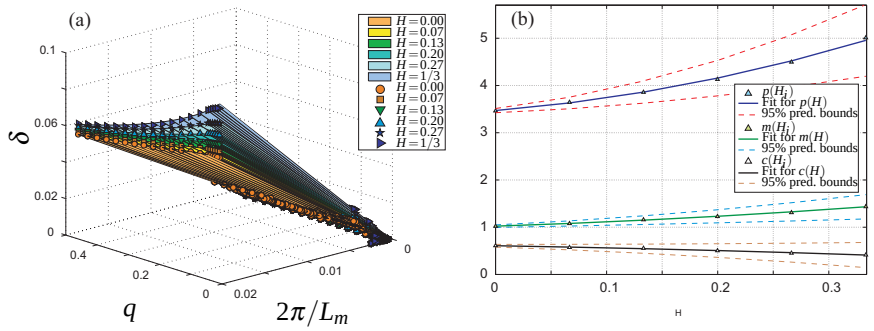

Fig. 9. The plotted points represents the changes in the maximum location with respect to the inverse of the adimensional scale, $2\pi/L_m$, and the scale ratio, q, for different values of H. The surface that fits these points follow Eq. (24) (extended figure in Media 1): $p(H) = 7.645(\pm 3.664)H^2 + 1.907(\pm 0.921)H + 3.470(\pm 0.045)$, $c(H) = -0.5989(\pm 0.599)H^2 - 0.3902(\pm 0.376)H + 0.6082(\pm 0.029)$, and $m(H) = 1.39(\pm 1.000)H^2 + 0.765(\pm 0.361)H + 1.023(\pm 0.026)$.

The position of the maximum for the covariance difference now depends on two scales: q and L_m. This surface is dependent on H as shown in Fig. 9. We calculated the maximum position for

#175466 - $15.00 USD Received 4 Sep 2012; revised 4 Nov 2012; accepted 15 Nov 2012; published 29 Nov 2012

some scale pairs $(q, 2\pi/L_m)$ for a set of Hurst exponents from 0 to $1/3$ with step $\Delta H = 0.0333$, a reasonably good fit for these surfaces is given by

$$d = p(H)\frac{\ell_0}{\cosh\left[m(H)\left(\frac{\ell_0}{L_0}\right)^{c(H)}\right]}, \tag{24}$$

where the fitting coefficients $p(H), m(H)$ and $c(H)$ can be modelled by quadratic polynomials, see Fig. 9(b). Likewise, the axis-cut for the on-plane covariance is a function of q and L_m. It is particularly sensitive to the values of the scale ratio; effectively, even the smallest departures from $q = 0$ produces an axis-cut function strongly dependent on the adimensional propagation distance, Fig. 10. This dependence recedes for larger adimensional scales when the scale-ratio takes values above 0.1, becoming almost constant for $L_m > 500$. Moreover, with this departure from small q-values the cuts for the different states of the turbulence coalesce to one surface. A simple fit, as in Eq. (24), is impossible. The best approximations require far more coefficients and complex functional relations. In any circumstance the axis cut is dependent of L, L_0, ℓ_0, and, of course, the Hurst exponent H. This implies that all the scales defining the cut are relevant; particularly, for realistic scale ratios ($q \leq 0.1$) a strong dependence on the inner-scale and propagation distance is found.

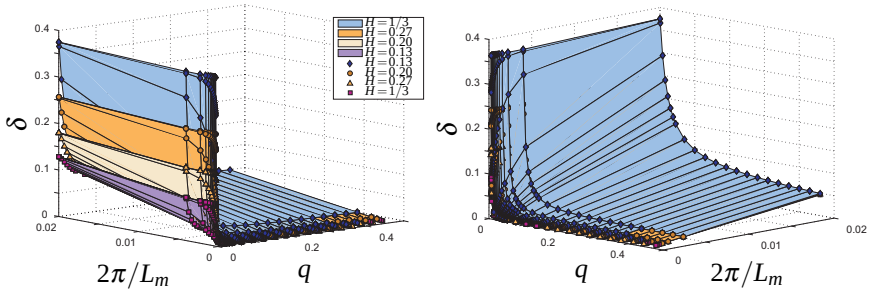

Fig. 10. The plotted points represents the changes in the axis-cut location with respect to the inverse of the adimensional scale, $2\pi/L_m$, and the scale ratio, q, for different values of H. Interpolant surface fits are used to exemplify its behaviour, a true interpolant function was not found (extended figure in Media 2).

4. Conclusions

Throughout this work we have given an exhaustive description for the GO approximation to the propagation of thin-beams through varied non-Kolmogorov models for the turbulent refractive index. Moreover, we have extended results obtained by pioneer works from Consortini *et al.* [7, 8] to any possible state of the turbulence. This is extremely important, since, as we discussed previously, deviations are expected for the range of usability of an experimental technique based in this theory—see again [12, 15–19].

We have confirmed the dependence of the wandering statistics of two parallels beams (on- and off-axis covariances) on the inner- and outer-scales, and the degree of development of the turbulence, H. In [8, 9] was shown that the characteristic scales of the optical turbulence could be determined from the topological characteristics of the correlation curves: the position of the maximum of Δ roughly determined the inner-scale, and the axis-cut in the on-plane covariance estimated the outer-scale. Nevertheless, in the present work we have given a more precise description of both characteristics; they are not only exclusive functions either of the inner-

#175466 - $15.00 USD Received 4 Sep 2012; revised 4 Nov 2012; accepted 15 Nov 2012; published 29 Nov 2012

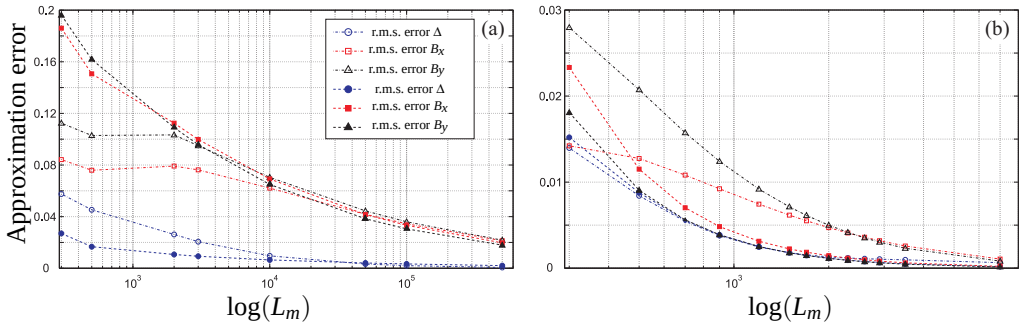

Fig. 11. Comparison between Consortini's asymptotic approximation and our numerical approach: (a) r.m.s. error for relative separation in $0 \leq \delta \leq 0.02$ (filled markers) and $0 \leq \delta \leq 0.4$ (hollow markers) in the Tatarskĭ case (Media 3); (b) r.m.s. error for relative separation in $0 \leq \delta \leq 0.02$ (filled markers) and $0 \leq \delta \leq 0.45$ (hollow markers) in the von Kármán case (Media 4). The L_2 norm is used as a measure of the uniform convergence (r.m.s error) in both cases.

or outer-scales, but they both depend on the value of H. The maximum in the covariance difference responds strongly to ℓ_0; although some correction is due to the scale ratio (up to 10%) larger deviations are entirely attributable to the degree of development of the optical turbulence. On the other hand, the axis-cut observed in the on-plane covariance is strongly affected by both ratios ℓ_0/L and q. The axis-cut alone is unable to provide an accurate estimate of the outer-scale (incidentally it exists regardless of the existence of L_0, Figs. 2 and 5), the inner-scale is necessary for the determination of the outer-scale, for any state of the turbulence. Experimentally, this restricts us from determining the scales independently from each other, at least not without error. Innocenti & Consortini [31] encountered this problem while comparing the Hill-Andrews spectrum with the von Kármán. Moreover, due to the dependence of these properties with H the state of the turbulence should be asserted by other means before attempting to estimate the scales.

Since the present approach provides exact numerical integration of the filter function, $\tilde{g}_n$ and $\tilde{f}_n$, it is particularly suitable for short-path distances found in the laboratory. Figure 11 exemplifies the asymptotic limit, for the Kolmogorov condition $H = 1/3$, to the long-path approximation obtained in [7]. The Tatarskĭ model requires high values of the adimensional distance ($L_m \geq 10^5$) to achieve low r.m.s. error—particularly for the normalized on- and off-plane covariances. For instance, this induces the absence of an axis-cut in the asymptotic approximation, see Fig. 11(a) (Media 3). On the other hand, the von Kármán model gives much better results: values for L_m larger than 10^3 provides good agreement between the Consortini's asymptotic approximation and our approach, Fig. 11(b). Disagreements on low values of the adimensional propagation are notable, this alters particularly the position of the axis-cut in the on-plane covariance, Fig. 11(b) (Media 4). On the contrary, the maxima of the covariance difference are extremely stable: the asymptotic approximation provides a formula identical to Eq. (24)—its coefficients are within the error margin of the ones given in our generalization for $H = 1/3$.

We have discussed the twin beams correlations under three different generalized spectra: (self-similar) non-Kolmogorov, (non-K) Tatarskĭ and (non-K) von Kármán. As it is well known, the von Kármán spectrum is the more general of the three, it has both scales present, and thus provides a more complete description of turbulent perturbations to the refractive index. Nevertheless, real turbulence is known to present a characteristic bump in the spectrum [30], as found in [31] the atmospheric spectrum provides a better representation of the experimental data for long propagation path. In future works we aim to study it through non-Kolmogorov

#175466 - $15.00 USD Received 4 Sep 2012; revised 4 Nov 2012; accepted 15 Nov 2012; published 29 Nov 2012

atmospheric spectrum, and elaborate comparisons with the results provided here.

Finally, we reserve a full analysis for the non-Kolmogorov spectrum on the effects of partially filled paths to a future work. We can anticipate what seems to be a general rule in this case. The fraction of static air p has a *lowering* effect on the covariances. The strength of the correlation is diminished by the unfilled region, and this has an effect on the position of the axis-cut but apparently has no influence on the position of the maximum. We have discussed this issue in [32], where we have applied successfully the methods presented here to the determination of inner- and outer-scales for turbulence generated in a small chamber of about 37 centimeters partially filling a propagation path of 1.29 m ($p = 0.71$); these scales are reproduced independently by other techniques. Further research should be done to establish the extent of its effect in any turbulence condition.

Acknowledgments

This work was supported by Comisión Nacional de Investigación Científica y Tecnológica (CONICYT, FONDECYT Grant No. 1100753, Chile), partially by Pontificia Universidad Católica de Valparaíso (PUCV, Grant No. 123.704/2010, Chile) and Consejo Nacional de Investigaciones Científicas y Técnicas (CONICET, Argentina).

#175466 - $15.00 USD Received 4 Sep 2012; revised 4 Nov 2012; accepted 15 Nov 2012; published 29 Nov 2012